Journal of Materials Chemistry B

Polymer Composition Primarily Determines the Protein Recognition Characteristics of Molecularly Imprinted Hydrogels

Journal:	*Journal of Materials Chemistry B*
Manuscript ID	TB-ART-07-2020-001627.R1
Article Type:	Paper
Date Submitted by the Author:	20-Jul-2020
Complete List of Authors:	Venkataraman, Abhijeet; University of Texas at Austin, Department of Biomedical Engineering Clegg, John; University of Texas at Austin, Department of Biomedical Engineering Peppas, Nicholas; The University of Texas at Austin, Chemical Engineering, Biomedical Engineering

Polymer Composition Primarily Determines the Protein Recognition Characteristics of Molecularly Imprinted Hydrogels

Abhijeet K. Venkataraman[1], John R. Clegg[1], and Nicholas A. Peppas[1,2,3,4,5,6*]

[1] Department of Biomedical Engineering, University of Texas, Austin, TX, 78712, USA

[2] McKetta Department of Chemical Engineering, University of Texas, Austin, TX, 78712, USA

[3] Institute for Biomaterials, Drug Delivery, and Regenerative Medicine University of Texas, Austin, TX, 78705, USA

[4] Department of Pediatrics, Dell Medical School, Austin, TX, 78712, USA

[5] Department of Surgery and Perioperative Care, Dell Medical School, Austin, TX, 78712, USA

[6] Division of Molecular Pharmaceutics and Drug Delivery, College of Pharmacy, University of Texas, Austin, TX, 78712, USA

**Correspondence to: peppas@che.utexas.edu*

Current Address (JRC): Harvard University / Wyss Institute for Biologically Inspired Engineering, 3 Blackfan Cir, Boston, MA, 02115, USA

Abstract

Synthetic hydrogels with the ability to recognize and bind target proteins are useful for a number of applications, including biosensing and therapeutic agent delivery. One popular method for fabricating recognitive hydrogels is molecular imprinting. A long-standing hypothesis of the field is that these molecularly imprinted polymers (MIPs) retain the chemical and geometric profile of their protein template, resulting in subsequent ability to recognize the template in solution. Here, we systematically determined the influence of network composition, as well as the identity, amount, and extraction of imprinting templates, on the protein binding of MIPs. Network composition (i.e. the relative number of ionizable and hydrophobic groups) explained the extent of protein adsorption in all

cases. The identity and amount of imprinting template, albeit a protein or synthetic polymer (PEG) of similar molecular weight, did not significantly influence the amount of protein bound. While the purification method influenced the extent of template adsorption, it did so by chemically modifying the network (acrylamide hydrolysis, increasing the acid content by up to 21%) and not by voiding occupied MIP pores. Therefore, our results indicate that material composition determines the extent to which MIPs bind template and non-template proteins.

Graphical Abstract:

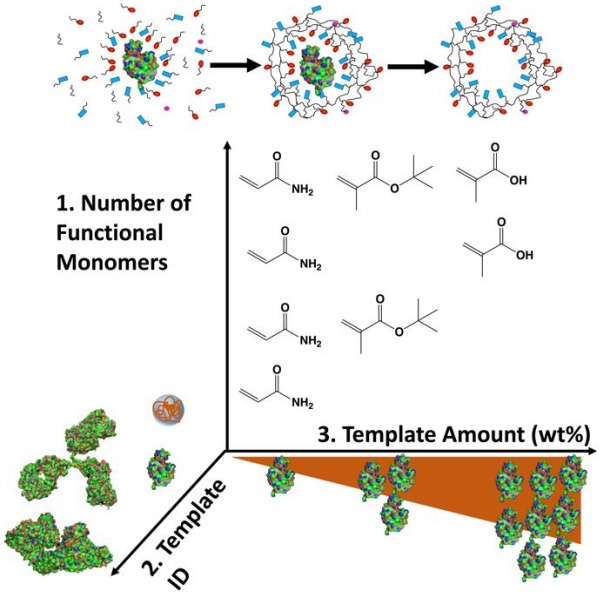

Keywords

Molecularly Imprinted Polymer, Hydrogel, Biosensor, Protein Adsorption, Molecular Recognition

Introduction

Biology has mastered systems for purposeful molecular recognition. Molecular recognition events, where ligand and receptor molecules bind with specificity, mediate numerous biological processes including but not limited to cell motility, proliferation, and surveillance. One approach in the realm of biomedical technology is to repurpose biological machinery as components of medical devices. Antibodies and enzymes for example, which are produced by biological systems and applied *ex vivo*, are recognitive agents for diagnostic biosensors. A second approach is to use the biological process as inspiration, and reverse-engineer materials that mimic protein recognition. While mimicking the complexity of protein recognition is challenging, synthetic materials have advantageous properties including their tunability and robustness to environmental conditions. Therefore, there is significant interest in fabricating synthetic, recognitive materials, and applying them as drug delivery vehicles[1–6], biosensors[7–9] and scaffolds for tissue engineering.[10,11]

One synthetic approach for generating biomimetic materials for protein recognition applications is molecular imprinting. Molecularly imprinted polymers (MIPs) are synthetic materials designed to mimic the antigen binding properties of antibodies.[12] In the synthesis of MIPs, templates (i.e. small molecules, proteins, cells), monomers, and crosslinking agents are incubated in aqueous buffer. During a pre-assembly step, non-covalent interactions form between template molecules and monomer functional groups.[5,6,13] After equilibrium association is achieved, an initiator is added, leading to the formation of crosslinked, multifunctional networks around the template.[14,15] Purification, through repeated washes, aims to remove all of the entrapped template, as well as

unreacted monomers.[16] The prevailing hypothesis of the field is that this template-guided synthesis–molecular extraction process generates pores that are complementary geometrically and chemically to the template, giving the MIPs the ability to recognize and specifically bind the template in biological fluids.

Numerous parameters must be optimized when designing and synthesizing a new MIP for protein recognition. The network mesh size must be sufficiently large to permit template diffusion but sufficiently small to hold the geometry of protein imprint. The electrostatic, hydrophobic, and hydrogen bonding interactions must be sufficiently strong to generate high affinity protein-polymer binding, but must be rendered weak by wash buffers in order to remove entrapped template. The combination and arrangement of functional groups within the MIP must be sufficiently specific, so that other ligands, such as salts, sugars, and other proteins, bind the MIP with a lesser affinity than the template. While a multitude of studies have investigated protein imprinting, and designed application-specific MIPs, the relative importance of each MIP design parameter (i.e. addition of functional groups, template identity, amount of template, template extraction) on the extent and specificity of protein absorption remains unclear.

A recent perspective by Culver and Peppas[12] called the core hypotheses of protein molecular imprinting into question, citing key elements of monomer-template self-assembly, MIP purification, and protein adsorption. Herein, new questions raised in their analysis are probed experimentally. We focused on determining the relative impact of 4 variables: composition, template identity, template quantity and template extraction, on the extent and specificity of protein adsorption to MIPs. We performed these analyses by synthesizing three unique libraries of MIPs and quantifying the extent and specificity of

protein adsorption to each library. In the first group, we varied composition by incorporating additional functional monomers (i.e. hydrophobic, anionic) within the MIPs. Next, we synthesized MIPs with model proteins that possessed a range of molecular weights and isoelectric points. Last, we varied the quantity of entrapped template, as well as the extent to which that template was extracted during purification. In each case, our dependent variable was the equilibrium adsorption of a range of model proteins (i.e. lysozyme, cytochrome c, hemoglobin, gamma globulin, albumin).

We hypothesized that composition would primarily dictate the physical (i.e. swelling, stiffness) and chemical (i.e. presentation of moieties which can engage a ligand in a favorable manner) properties of hydrogel MIPs. However, we also anticipated that the templating process would impart specific protein adsorption properties. If in fact the imprinting process imparts template specificity, then we hypothesized that the amount of entrapped template, as well as extent of template extraction during purification, would influence the protein binding properties of the resulting MIP.

Experimental

Materials. All chemicals were purchased from Sigma-Aldrich or Thermo Fisher Scientific and used as received. Ultrapure water (18.2 MΩ · cm) was obtained from a GenPure Pro system (Sigma).

Synthesis of MIPs and NIPs. For the synthesis of MIP and NIP hydrogels, acrylamide (AAm), methacrylic acid (MAA), and tert-butyl methacrylate (tBMA) were selected as monomers. They were crosslinked with N,N'-methylene bisacrylamide (Bis). Irgacure 184 (1-hydroxycyclohexyl phenyl ketone) was used as a photoinitiator. Protein templates for

the MIPs were lysozyme from chicken egg white (Lys/L), hemoglobin from bovine blood (HGB/H), γ-globulin from bovine blood (Glob/Y), and albumin from bovine serum (BSA/B). As a control, to look at porogenic effects of templating without protein specificity, we also fabricated MIPs with polyethylene glycol (MW = 10 kDa) (PEG) as a template. These templates have differing properties, shown in **Table 1.** In our naming convention, the template identity is listed at the end of the formulation name.

Table 1: Protein identities and physicochemical properties. Templates were classified by their molecular weight and isoelectric point. Three model proteins (Lysozyme, γ Globulin and BSA) were selected as imprinting templates because of their prevalence in existing molecular imprinting literature, as well as their range of size and extent of ionization in physiologically relevant buffers. PEG was used as a control (non-protein) template. Cytochrome c and hemoglobin were used in protein adsorption experiments.

Template/Protein	Molecular Weight (kDa)	Isoelectric Point (pI)
Lysozyme[17]	14.3	11.3
γ Globulin[18,19]	157.5	6.9
BSA[20,21]	66.4	4.8
Hemoglobin[22]	64.5	6.8
Cytochrome C[23]	12.4	9.6
PEG	10	–

Four homopolymers or copolymers were synthesized: P(AAm), P(AAm-co-MAA), P(AAm-co-tBMA) and P(AAm-co-MAA-co-tBMA). All mole and weight percentages are presented as their percent of the total monomer/crosslinker feed. All hydrogels contained 2 mol% Bis crosslinker and 0.5 wt% Irgacure 184. In all cases where MAA was added, it was included at 25 mol%, while tBMA was added at 15 mol%. Each pre-polymer solution contained 1 g of monomer and crosslinker. The monomers, crosslinker, and photoinitiator were dissolved at 40 wt% in a 50/50 v/v mixture of water/ethanol. Each formulation was synthesized in five unique ways: without template (NIP), or with one of four protein templates: Lys (LMIPs), HGB (HMIPs), Glob (YMIPs) or BSA (BMIPs). For each MIP, 20

mg of template were added to the pre-polymer solution (2 wt%, relative to monomer). For control NIPs, 20 mg of water were added.

Each MIP or NIP was synthesized in a nitrogen environment (MBRAUN Glovebox), void of oxygen and water vapor, which was maintained at 25 ˚C. Monomer solutions were purged for five minutes with a steady flow of nitrogen to remove dissolved oxygen, then pipetted between glass plates separated with a 0.7 mm Teflon spacer. Polymerization was initiated by UV exposure at 365 nm (18 $mW \cdot cm^{-2}$, 20 min) (Dymax 2000-EC Light Curing System). Separately, a library of gels with a range of template inclusion were synthesized. These gels (P(AAm) or P(AAm-co-MAA-co-tBMA) each crosslinked with 2 mol% Bis, 3 g total monomer, 40 wt% monomer in water/ethanol, 0.5 wt% Irgacure 184) were synthesized as described above, but contained a varying amount (0 to 10% of pre-polymerization weight of total solution) of Lys or PEG (MW = 10 kDa) as a template.

MIP and NIP Purification. To remove any unreacted monomer and template, all hydrogels were washed against a water/ethanol gradient starting at 1:1 water: ethanol ratio (subsequent washes were 3:1, 7:1, and 15:1 water: ethanol, followed by ultrapure water). Each wash was at least 24 h in duration and was replicated twice. To determine the impact of the extent of template extraction on protein adsorption, the MIPs fabricated with a range of Lys or PEG template were split into three groups: control, EDTA and Trypsin-EDTA. For the control group, no extra washes were done, and the majority of the template remained. For the ETDA group, the hydrogels were washed with 1M EDTA pH 8.0 (4 washes, 24 h each), transferred to 1x PBS pH 7.4 (4 washes, 24 h each), and then ultrapure water 4 times. The purpose of this purification series was to elute entrapped template by competing for protein-MIP electrostatic interactions with a multivalent anion.

Effectively, this removed most, but not all, of the entrapped template. The MIPs in the final group, Trypsin-EDTA, were first washed with 0.25 wt% porcine trypsin dissolved in 1 M EDTA pH 8.0 (4 washes, 24 h each), followed by the full EDTA protocol (EDTA 4 washes, PBS 4 washes, Water 4 washes). This group used template digestion by trypsin, followed by ionic competition, as a method for extracting the entirety of entrapped template. A full graphical summary of all MIP fabrication and purification variants is presented in **Figure 1.**

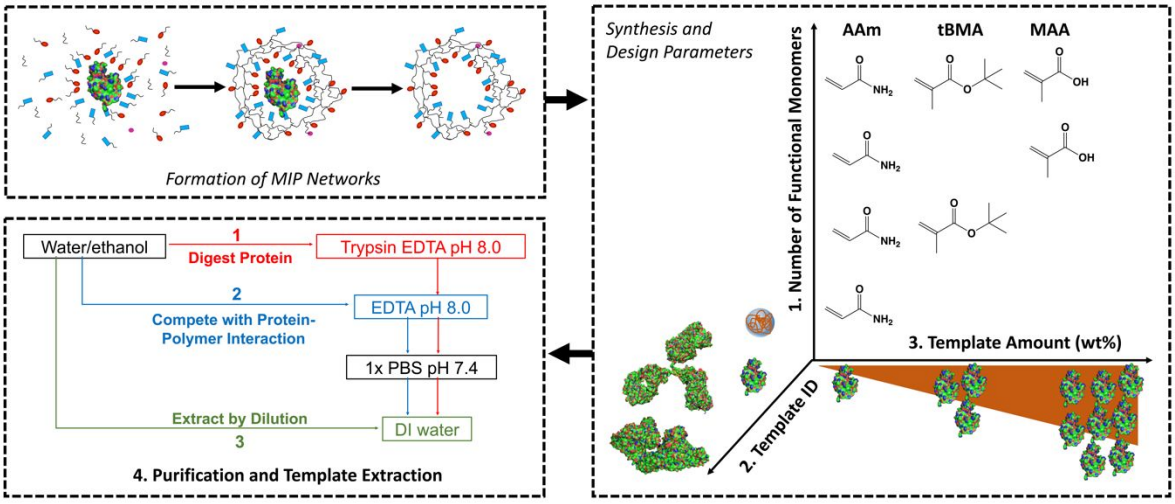

Figure 1: Schematic of the polymerization and purification of the Molecularly Imprinted Polymers (MIPs). MIPs were fabricated via the self- assembly and photopolymerization of functional monomers (AAm, MAA, tBMA) around a molecular template (BSA, gamma globulin, lysozyme, poly(ethylene glycol)). The 4 different variables explored are shown: MIP polymeric composition, template identity, amount of template, and purification method / extent of template extraction. In each case, our dependent variable of study was the equilibrium adsorption (in relative dry mass) of template and non-template proteins.

Fabrication of MIP discs and microparticles. After purifying the MIPs, 10 mm discs were punched from the swollen hydrogels using a cork borer. The MIPs were then allowed to dry under ambient conditions, followed by complete drying under vacuum (> 72 h, 37 °C). After this, a portion of each MIP or NIP was manually crushed into microparticles using a mortar and pestle, and the fraction with a diameter of no more than 45 μm was

collected through a sieve. The 10 mm discs were used for swelling studies. All other experiments utilized the crushed microparticles. For subsequent protein adsorption experiments, the MIPs and NIPs were reconstituted at 1 mg/mL (dry polymer weight in water) and adjusted with 1 N NaOH to a final pH of 7.4 ± 0.05. During the pH adjustment, the MIP and NIP suspensions were allowed to equilibrate for several hours, to ensure a stable pH mimicking physiological conditions. This ensured that the MIPs and NIPs were in a fully water-swollen state, with a similar extent of MAA deprotonation, for all protein binding experiments.

Scanning Electron Microscopy. SEM studies were conducted on the MIP and NIP microparticles using a Zeiss Supra 40V Scanning Electron Microscope, with a working distance of 30.2 mm and voltage of 5 kV. The images collected had variable magnification, which is given on each image.

Fourier Transform Infrared Spectroscopy. ATR-FTIR spectroscopy studies were conducted on all hydrogels using a Nicolet is10 ATR-FTIR with germanium crystal (Thermo Fisher Scientific). The data presented focus on the instructive wavenumber range of 2000 to 1000 cm^{-1}.

Potentiometric Titration. The amount of methacrylic acid incorporated into the MIPs was determined by potentiometric titration. Ten milligrams of polymer were suspended in 60 mL of 5 mM KCl buffer, and adjusted to pH = 10 with 1 N NaOH. Pure KCl buffer, without polymer, was used as a control. All samples were titrated with 0.01 N HCl solution using a Hanna H1901C autotitrator until they reached pH = 3. The amount of methacrylic acid was computed using the following equation, described previously[24]:

$$m_{MAA} = \frac{1}{0.499}(V_s - V_b) \times N_{titrant} \times MW_{MAA}$$

where m_{MAA} is the mass of methacrylic acid incorporated in the microparticles, m_p is the mass of microparticles in solution (0.01 g), V_s is the volume of acid added to titrate the samples from pH 7.8 to pH 4.8, V_b is the volume of acid added to titrate the pure 5 mM KCl sample from pH 7.8 to pH 4.8, $N_{titrant}$ is the normality of the titrant (0.01 N) and MW_{MAA} is the molecular weight of the MAA monomer (86.06 g/mol).

Equilibrium Film Swelling. Swelling studies were conducted in 1x PBS. First, individual discs were weighed for their dry weight. These discs were then allowed to swell to equilibrium in 5 mL of 1x PBS (24 h), and were weighed again. The mass swelling ratio was then computed using the following equation:

$$q = \frac{m_s}{m_d}$$

where q is the mass swelling ratio, m_s is the mass of the swollen disc and m_d is the mass of the dry disc.

Unextracted Protein. The protein remaining within MIPs was quantified using a microBCA assay (Thermo Fisher Scientific) as described previously.[25] MIP or NIP microparticles (1 mg/mL in 1x PBS, pH = 7.4) were mixed in equal volume ratio with microBCA reagent and incubated at 37 °C for 2 h on an orbital shaker to allow any protein entrapped within the MIP to induce a colorimetric change in the supernatant. Then, the samples were centrifuged at 15,000g for 7 min. The protein content was determined by the color change in the supernatant (λ = 562 nm), as compared to standards prepared for each template protein.

Protein Binding. Five model proteins – Lys, HGB, Cytochrome C from equine heart (Cyt C), Glob and BSA – were used to assess the specificity and intensity of the interactions between the various MIPs and various proteins. All proteins and MIPs were dissolved in 1x PBS at 1 mg/mL. For each of the protein-MIP pairs, the solutions were combined at equal volume (Final concentrations: 0.5 mg/mL protein, 0.5 mg/mL MIP), which were allowed to mix end-over-end for 1 h at room temperature. The samples were pelleted by centrifuging at 15,000g for 7 min.

For Lys, HGB, Cyt C quantification, the supernatants' absorbance was measured at 280 nm (Lys) and 405 nm (HGB, Cyt C). Unbound protein was quantified by comparing the supernatant absorbance to a protein-specific standard. For Glob and BSA, the supernatant (15 µL) was diluted in 1x PBS at pH = 7.4 (135 µL) and microBCA working reagent (150 µL) and pipetted in 96 well microplates. These samples were then incubated at 37 °C for two hours on an orbital mixer. The absorbance of each sample was read at 562 nm and compared to protein-specific standards.

From the supernatant protein concentrations at equilibrium, we calculated the absorption capacity of the MIPs for each of the proteins using the following expression:

$$Q = \frac{(C_0 - C_e)V}{m}$$

where Q is the normalized mass bound, in mg of protein per g of microparticles. Further, C_0 is the initial protein concentration (0.5 mg/mL), C_e is the equilibrium protein concentration in the supernatant (variable), V is the solution volume (0.6 mL) and m is the mass of microparticles (0.0005 g).

Statistical Analysis. All studies were conducted with in at least triplicate. Results are presented as mean ± standard deviation. All results were analyzed using a two-way ANOVA and pairwise comparisons were performed with Dunnett's test in GraphPad Prism. Statistical significance is indicated on figures using: *$p < 0.05$, **$p < 0.01$, ***$p < 0.001$.

Results & Discussion

Characterization of the Hydrogels. All microparticles were random and non-spherical in geometry, as well as similar in diameter, as a result of the crushing and sieving process. Microparticle diameter and morphology were observed using SEM (**Figure 2a, S1-S4**). The dried microparticles had an irregular geometry and porous structure. There were no apparent differences the morphology of microparticle samples comprised of P(AAm) (**Figure S2**), P(AAm-co-MAA-co-tBMA) (**Figure S3**) or MIPs fabricated with different templates (**Figures S3 and S4**). This result contrasts some previous studies, which have shown that the presence of template during synthesis can alter the MIPs' morphology[26], and demonstrates that, depending on polymer fabrication and processing conditions, imprinting can but does not necessarily alter particle morphology.

The incorporation of all feed monomers was validated using FTIR spectroscopy. Spectra were collected on vacuum dried MIP and NIP microparticles from 600 to 4000 cm^{-1}. We specifically analyzed the wavenumber range of 1000 to 2000 cm^{-1} to identify the characteristic peaks for the amide carbonyl (1660 cm^{-1}) (AAm and Bis), and the methacrylate ester (1150 cm^{-1}) (tBMA and MAA). The FTIR data indicated that all feed monomers were incorporated in all formulations (**Figure S5**). As expected, template

identity did not significantly affect microparticle composition (**Figure S5**), even when up to 10 wt% template was added (**Figure S6**).

In two of our purification processes (EDTA, Trypsin EDTA), the hydrogels were washed in buffers with a pH equal to or greater than 7.4 following synthesis but prior to drying. We wanted to ensure that these purification conditions (i.e. pH, introduction of salts or enzymes) were not unnecessarily modifying the chemical composition of the MIPs or NIPs. As shown in **Figure S7,** there were differences in the FTIR absorbance spectra for vacuum dried hydrogels purified by the three different methods (control, EDTA method and Trypsin-EDTA method) at 1730 cm^{-1} (carboxyl carbonyl, protonated), 1550 cm^{-1} (carboxylate ion, deprotonated), and 1150 cm^{-1} (carboxylate ester). MIPs washed with EDTA or Trypsin-EDTA had a greater carboxylate ion absorbance but a lesser carboxyl carbonyl and carboxylate ester absorbance. This motivated further investigation, to determine if this difference was due to carboxylic acid protonation / deprotonation, or was a result of MIP chemical modification.

Poly(methacrylic acid) (PMAA) has a pK_a of about 4.8 ± 0.5.[27] We performed potentiometric titrations on microparticles composed of P(AAm-co-MAA-co-tBMA), washed by each of the three methods, to calculate the amount of MAA present in the sample (**Figure S8**). Relative to the amount of methacrylic acid in the monomer feed, MIPs washed with water only had 99% of the expected acid content (25 mol%, from the monomer feed), as compared to 110% for the EDTA method and 120% for the Trypsin-ETDA method. This indicated that the majority of the difference observed in the FTIR spectra were due to differences in MAA protonation, from prolonged incubation in slightly basic buffer (pH = 7.4 to 8). The increase in acid content (up to a 21% increase), as a

result of the purification method, was likely due to acrylamide hydrolysis, as we have shown previously.[28–30] The FTIR absorbance peak corresponding to the amide carbonyl had the greatest intensity in all formulations (1660 cm^{-1}), indicating that the majority of the acrylamide remains unmodified following each of the three purification methods.

Hydrogel Characterization by Equilibrium Swelling. Another key physical property of the hydrogels is their mesh size.[31] The hydrogel mesh size, ξ, which is defined as the diameter of the largest solute which can pass through the network, is inversely related to the polymer volume fraction in the swollen state $v_{2,s}$.[32,33] When the polymer volume fraction is greater than 10%, as was the case in this study, this mesh size scales with the equilibrium swelling ratio, q.

$$\xi \sim v_{2,s}^{-1} = q$$

The swelling ratio is influenced by a number of hydrogel design parameters. The hydrogel composition, as determined by the monomer feed and relative incorporation, determines the thermodynamic compatibility of the polymer-water interaction (i.e. the polymer-solvent Flory interaction parameter, χ).[34,35] The swelling ratio is also influenced by the molecular weight between crosslinks, the pH and ionic strength of the medium, and the acid dissociation constants, K_a, for any ionizable subunits (e.g. MAA).[36] In addition to determining the size of the network mesh, the equilibrium swelling ratio provides a surrogate measure of the maximum volume for protein binding (i.e. the number and availability of binding sites).

In the present study, we altered each hydrogel's physical properties by (i) incorporating different co-monomers, (ii) including template molecules, and (iii) extracting

the entrapped template to different extents. We quantified the equilibrium swelling ratio of each formulation (**Figure 2**) to determine the extent to which each MIP design parameter influenced the mesh size.

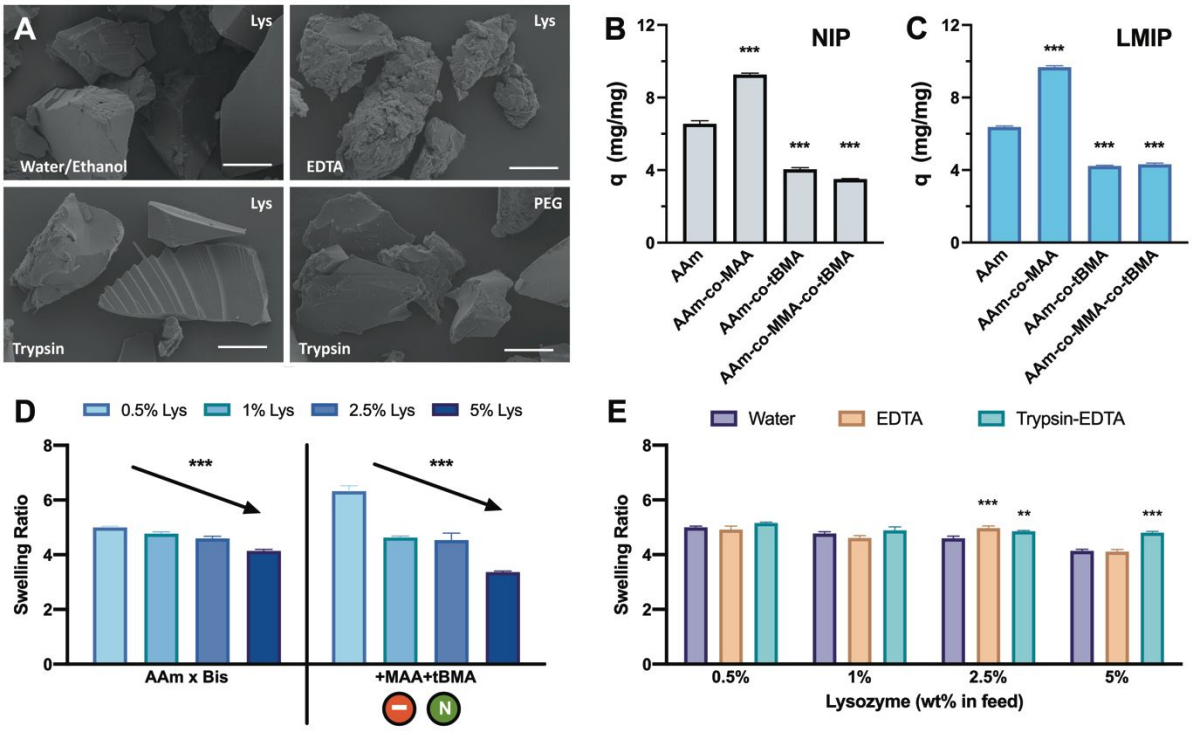

Figure 2: **Characterization of MIP and NIP Hydrogels (a)** SEM analysis of P(AAm-co-MAA-co-tBMA) MIP microparticles, following synthesis and purification. Listed in the bottom left of each image is the purification method, and the top right is the template identity (5 wt%). SEM images collected at a working distance of 30 mm and 2,000x magnification. Scale bar = 25 μm. **(b)** The addition of MAA to the formulation significantly increased the swelling ratio in 1x PBS, while the addition of tBMA decreased the swelling ratio. Co-polymer NIPs with AAm, MAA and tBMA swelled similarly to the formulation with AAm and tBMA. Denotations of statistical significance are relative to AAm only, as quantified by one-way ANOVA with multiple comparisons. **(c)** Lysozyme MIPs of each formulation exhibited similar swelling in 1x PBS to NIPs. **(d)** As the amount of added template (lysozyme) increased, the swelling ratio decreased (MIPs purified by dialysis only). Similar trends were exhibited by the P(AAm) formulation and the terpolymer gel containing MAA and tBMA. Statistical significance represents the significant trend in swelling ratio, with respect to the amount of template, determined by 2-way ANOVA. **(e)** When greater amounts template were extracted (i.e. by Trypsin-EDTA washing) from the 2.5 wt% and 5 wt% lysozyme MIPs, the swelling ratio in 1x PBS increased, relative to the dialysis-only purification (P(AAm) formulation shown). The significance shown is relative to the corresponding water control. (Data shown as mean ± SD, n = 3-12, *p < 0.05, **p

< 0.01, ***p < 0.001, unless specified, by 2-way ANOVA with Dunnett's posttest for multiple comparisons).

The presence of MAA or tBMA in NIPs **(Figure 2b)** or MIPs **(**Lys MIPs shown, **Fig 2c)** significantly influenced the mass swelling ratio in 1x PBS. Incorporation of MAA increased the swelling ratio by 66.4 ± 22.7% while the presence of tBMA decreased the swelling ratio by 29.9 ± 8.4%, relative to crosslinked acrylamide gels (average and standard deviation are presented for NIP, LMIP, YMIP, and BMIP). The combination of MAA and tBMA resulted in a 35.4 ± 8.3% decrease in swelling ratio, similar to the formulation with only tBMA added. The swelling ratio decreased as the amount of template present during the polymerization of AAm or AAm–co–MAA–co-tBMA was increased ($p < 0.001$ in both cases) **(Figure 2d)**. When that template was extracted completely through washes in trypsin and EDTA buffer, the swelling ratio increased **(Figure 2e),** although the magnitude of that increase was quite small (between zero and 16.1 ± 9.1%) when compared to the increase in swelling ratio due to MAA incorporation.

Therefore, the addition of ionizable and hydrophobic co-monomer was the main predictor of MIP or NIP swelling ratio. Complete template extraction with the trypsin and EDTA increased the swelling ratio, relative to control MIPs washed only with water. However, the magnitude of this increase was much less than that resulting from co-monomer incorporation.

Effect of Composition on Protein Absorption and Recognition. After characterizing the physical properties of the MIPs, we assessed their recognitive properties through equilibrium protein adsorption. For the MIPs and NIPs containing various templates at 0.8 wt% of the prepolymer solution, the adsorption of 5 proteins with varying size and isoelectric point was measured (**Table 1**).

First, we measured the equilibrium adsorption of each model protein to NIPs, to determine the influence of polymer composition, in the absence of molecular imprinting, on the extent of protein adsorption. NIP composition determined the quantity of Lys, Cyt C and HGB which bound at equilibrium **(Figure 3)**. The incorporation of hydrophobic interactions through tBMA, alone or in combination with MAA, did not increase the extent of Cyt C binding. The incorporation of tBMA increased HGB adsorption, and this increase was diminished through co-polymerization with MAA. This can be explained by the hydrophobic amino acid content of HGB[37], in combination with its slightly anionic charge at physiological pH, which will result in Coulombic repulsion from the anionic MAA copolymers. Uniquely, in the case of lysozyme; MAA and tBMA synergistically increased the magnitude of protein adsorption.

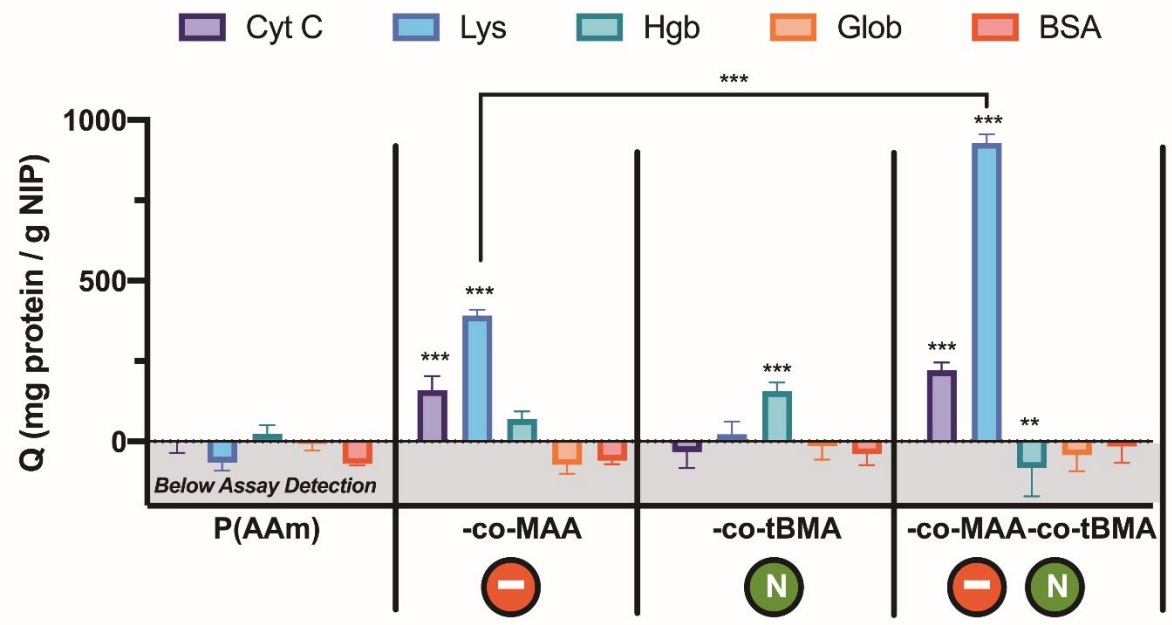

Figure 3: Five model proteins were bound individually to NIPs in 1x PBS at pH = 7.4. In particular, the data illuminate the impact of adding anionic groups (MAA) or hydrophobic moieties (tBMA), separately or in synergy, on the equilibrium adsorption of proteins ranging in molecular weight and isoelectric point. Coulombic interaction largely determined the extent and specificity of protein adsorption. Both cationic proteins (Cyt C, Lys) bound in significant quantity to all of the anionic NIPs. No protein tested bound in

detectable quantity to the base AAm x Bis formulation. Similarly, none of the anionic proteins (Glob, BSA) bound to any formulation tested. Only HGB adsorption was increased through hydrophobic interaction in the absence of charge interaction. Only in the case of lysozyme were the charge and hydrophobic interactions synergistic. (Data presented as mean ± SD, n = 3, **p < 0.01, ***p < 0.001, 2-way ANOVA with Tukey posttest).

Both Glob and BSA absorption were not influenced by NIP composition. Due to their low isoelectric point, Glob and BSA possess a negative charge at physiological pH and therefore cannot engage in complementary charge interactions with any of the tested formulations. As demonstrated in the case of both Lys and Cyt C, the addition of Coulombic interactions (through MAA co-polymerization) significantly increased the extent of protein adsorption.

The results presented in **Figure 3** indicate that MAA and tBMA altered the extent and specificity of Lys adsorption by contributing charge and hydrophobic interactions, not by altering the NIPs' swelling. As described in the previous section, NIPs with MAA and tBMA swelled to a lesser extent in 1x PBS than those with MAA only, yet they bound as much or more Cyt C and Lys. This indicated that specific intermolecular interactions, not transport limitations, determined protein adsorption to this library of NIPs.

We found that the presence or absence of Coulombic interactions between the model proteins and copolymers largely determined the extent of adsorption to each NIP. This finding is consistent with existing literature on recognitive biomaterials.[38] Hydrophobic interactions alone were particularly useful for enhancing absorption of HGB, a phenomenon unique to this work. The synergy of electrostatic and hydrophobic interactions, to increase protein absorption, was particularly evident in the case of Lys. This result is also consistent with previous literature on MIP systems.[39] Thus, in this work

we have confirmed that the identity and relative quantity of charged and hydrophobic subunits (i.e. moieties, monomers) is a critical consideration for MIP design.

Effect of Template Identity on Protein Absorption and Recognition. MIPs of each composition (AAm, AAm-co-MAA, AAm-co-tBMA, AAm-co-MAA-co-tBMA) were synthesized with each of the three protein templates (**Table 1**). The trends in model protein adsorption demonstrated by NIPs were also seen in each corresponding MIP. The mass of each model protein bound to each formulation was measured, to understand the impact template identity on protein adsorption (**Figure 4a,c and Figure S10**). Protein templating failed to improve the adsorption of any model protein to any formulation, as compared to non-imprinted particles of the same composition. Further, when template identity and MIP composition were treated as grouped independent variables in 2-way ANOVA, template identity accounted for less than 2% of the variation in model protein adsorption (all tested proteins). Composition accounted for more than 80% of the variation in adsorption (Lys, Cyt C, and HGB). This indicated that there was no significant relationship between template identity and subsequent molecular recognition, and that composition alone determined the protein-MIP affinity.

This result is consistent with some of those reported recently.[40] However, numerous other studies have shown new or enhanced protein-recognition behavior as a result of molecular imprinting. Given that imprinting failed to impart specific protein affinity for any template or MIP composition that we tested, when 0.8 wt% template was included, we hypothesized that differences in literature reports were due to differences in the amount of included or extracted template. After our initial synthesis and purification process, we noted that up to 1.6 wt% of the purified MIP was entrapped template. The

amount of template remaining differed as a function of template identity and MIP composition (**Figure 4 b,d**), but composition alone, irrespective of molecular imprinting, predicted the extent of model protein adsorption. Therefore, we hypothesized that template retention and the specificity of MIPs for free template molecules were not related. We next needed determine the influence of the amount of template included during synthesis, and extracted during purification, on the extent and specificity of model protein adsorption.

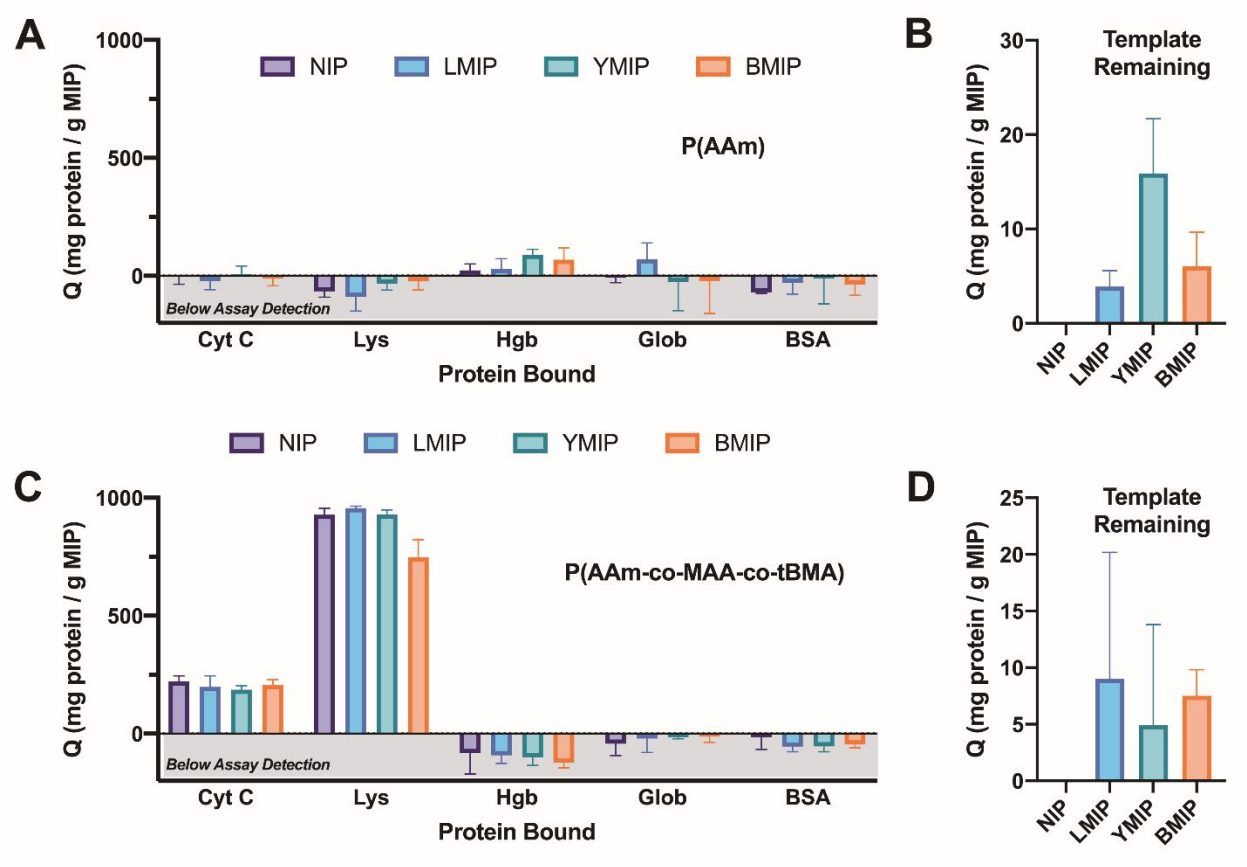

Figure 4: Normalized mass bound (Q) was computed for each of the 20 hydrogels (15 MIPs, 5 control NIPs) for 5 model proteins that varied in molecular weight and isoelectric point. **(a)** The adsorption of all tested proteins was negligible to MIPs and NIPs that lacked ionic and hydrophobic co-monomer, irrespective of template. **(b)** Template was retained in all MIPs, and varied as a function of template identity. **(c)** The amount of protein bound at equilibrium to terpolymer networks of AAm, MAA, and tBMA varied, and depended on the protein identity but not the MIP template identity. **(d)** Lysozyme, gamma globulin, and

BSA templates were similarly retained by terpolymer MIPs. (data presented as mean ± SD, n = 3)

Influence of Template Content on Protein Recognition. MIPs were synthesized (P(AAm) or P(AAm-co-MAA-co-tBMA) each crosslinked with 2 mol% Bis) with varying amounts (0.5 wt% to 5 wt%) of Lys or PEG. The MIPs were dialyzed against a water/ethanol gradient to remove all unreacted monomers and some entrapped template. After synthesizing, purifying, and reconstituting these new MIP hydrogels in 1x PBS, model protein adsorption experiments were conducted as described above, omitting HGB, Glob and BSA due to their negligible adsorption to the formulations interest (as shown previously in **Figures 3 and 4**).

Cyt C adsorption was not influenced by the extent (0.5 to 5 wt%) of Lys template (both for P(AAm) and P(AAm-co-MAA-co-tBMA) hydrogels) **(Figure 5a)**. Lysozyme adsorption was negatively related to the amount of template (P(AAm-co-MAA-co-tBMA) hydrogel) **(Figure 5b)**. This trend was the opposite of our expectation. However, microBCA analysis revealed that a significant amount of lysozyme remained following dialysis, which could explain why the absorption decreased **(Figure 5c)**. This led to looking for better purification methods, particularly those that remove all the remaining template.

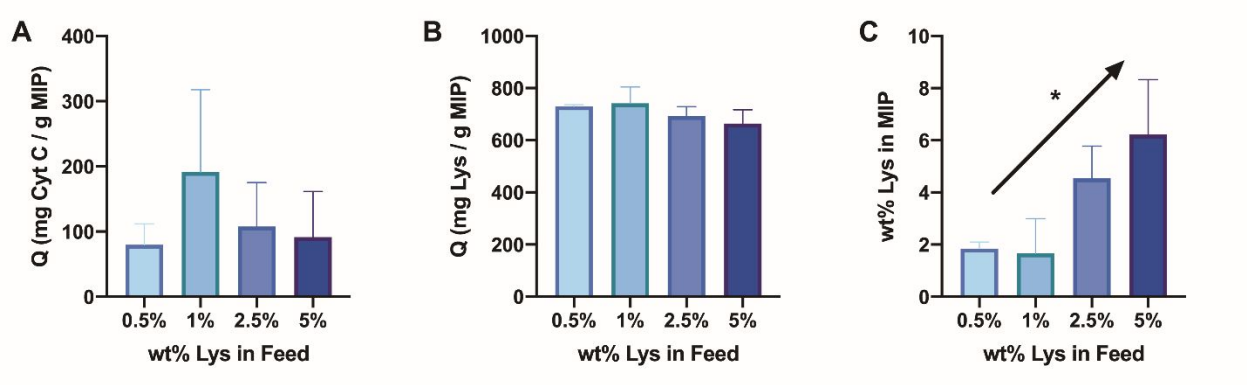

Figure 5: Protein adsorption to, and lysozyme template remaining within, Lys MIPs with different amounts of template. **(a)** The amount of lysozyme template did not impact Cyt C adsorption. **(b)** As the amount of lysozyme template increased, the amount of bound lysozyme at equilibrium decreased slightly, although the decrease was not significant statistically. **(c)** The amount of lysozyme retained after dialysis against water/ethanol was linearly related to the amount included during synthesis. (*$p < 0.05$ for the significance of the trend, one-way ANOVA) (all data presented as mean ± SD, n = 3)

Effect of Template Extraction on Protein Absorption and Recognition. We determined the influence of the extent of template extraction on protein recognition by MIPs. Two new purification methods were used (EDTA, Trypsin/EDTA), as described in the methods. Lysozyme MIPs, as well as PEG MIPs (template control) were polymerized with differing amounts of template (Lys or PEG, 0.5 to 5 wt%), and purified by a Trypsin/EDTA, EDTA, or water/ethanol protocol. Model protein absorption (Lys and Cyt C) was measured.

The three washing methods were successful in extracting different amounts of template. Lysozyme remained in all Lys-templated formulations washed with a water/ethanol gradient alone, and the amount of lysozyme remaining scaled linearly with the amount present during synthesis. On the other hand, lysozyme remained in the 2.5 at 5 wt% Lys MIPs washed in EDTA buffer. No retained protein was detected in MIPs washed with trypsin in EDTA buffer, followed by EDTA buffer **(Figure S11)**.

Lysozyme adsorption increased by an average of 14% as a result of washing with EDTA or Trypsin/EDTA, as compared to the same MIPs washed with water/ethanol. No difference was observed in lysozyme adsorption between MIPs washed by the EDTA or Trypsin/EDTA methods. Interestingly, this increase in Lys adsorption was not due to relative template extraction. Once all of the template was extracted (Trypsin-EDTA condition), no differences were observed in Lys adsorption for all tested formulations (0.5 to 5 wt% template) **(Figure 6a)**. Further, MIPs with PEG template, bound lysozyme in similar quantity **(Figure 6c)** to MIPs fabricated with lysozyme template. Purification method did not significantly influence the absorption of Cyt C **(Figure 6b),** and no difference in Cyt C adsorption was observed between MIPs with lysozyme or PEG templates **(Figure 6d)**. Similar trends were observed in lysozyme adsorption to P(AAm) MIPs, with the same initial template percentages and washing conditions **(Figure S12).**

The three purification methods, tested here, achieved their purpose of removing different amounts of the entrapped lysozyme template. However, template extraction did not result in new molecular recognition properties, as the relative adsorption of lysozyme and cytochrome c were not influenced by template extraction. Rather, the process of washing the P(AAm-co-MAA-co-tBMA) hydrogels increased lysozyme, but not cytochrome c, adsorption generally and independently of the amount of extracted template. In the materials characterization section, we determined that EDTA or Trypsin/EDTA washing increased the acid content of the MIPs by up to 21% through acrylamide hydrolysis. The fact that lysozyme adsorption increased as a result of EDTA or Trypsin/EDTA, irrespective of template identity or amount, is consistent with our

functional hypothesis that the extent of lysozyme adsorption is determined by network composition and not molecular imprinting.

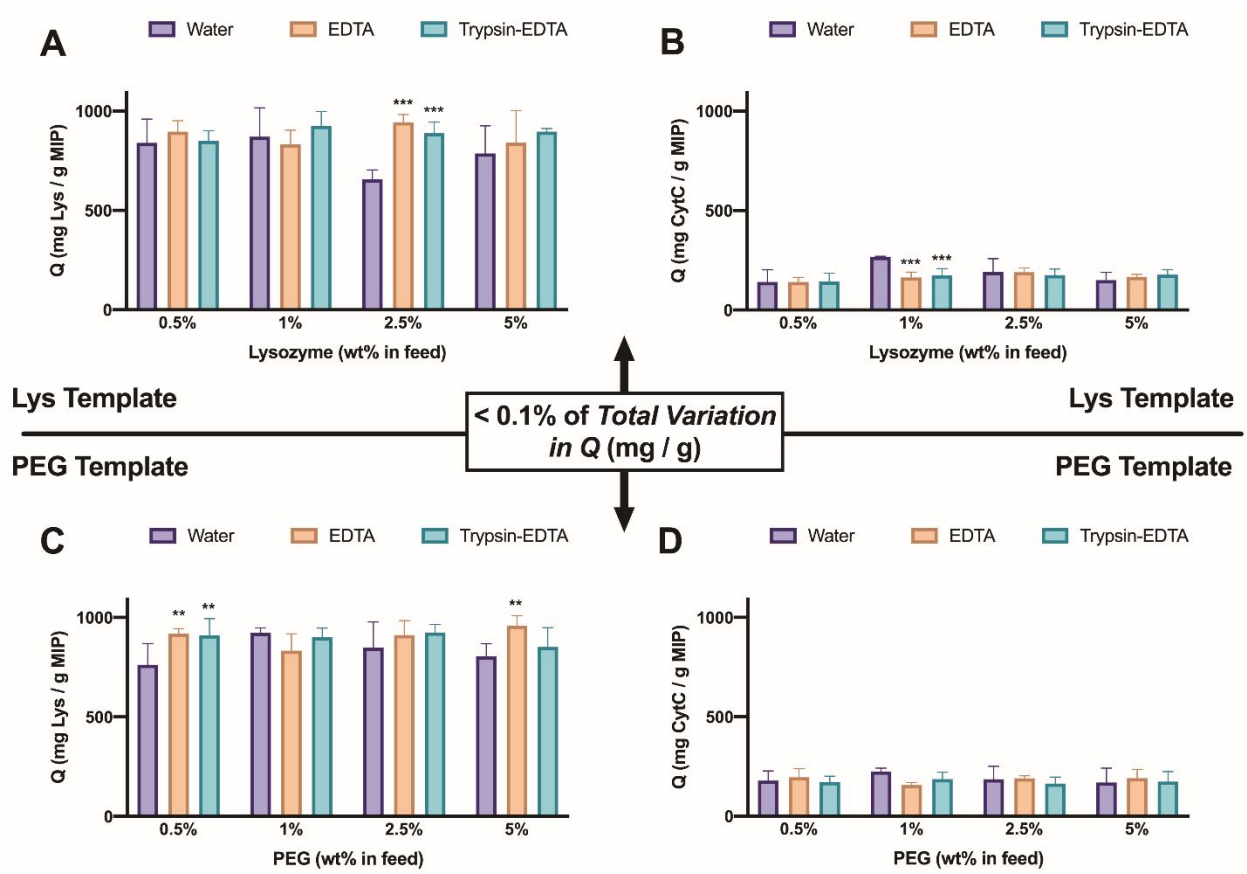

Figure 6: Impact of the extent of template extraction on the amount of Lys bound at equilibrium. **(a)** Lysozyme binding to Lys MIPs was increased by an average of 14% and up to 44% as a result of repeated MIP washing in EDTA or Trypsin EDTA buffer. (***p < 0.001, relative to corresponding 'water' formulation). **(b)** Cytochrome C adsorption to Lys MIPs was not enhanced by either purification methods (***p < 0.001, relative to corresponding 'water' formulation). **(c)** Lysozyme adsorption to PEG MIPs was enhanced by washing in EDTA or Trypsin/EDTA in a manner similar to the Lys MIPs (**p < 0.01, relative to corresponding 'water' formulation). **(d)** Cytochrome c adsorption to PEG MIPs was unaltered by purification method. When all data were lumped, treating the formulation/purification pair and template as independent variables and the mass protein bound as the dependent variable, less than 0.1% of the total variation in protein bound was explained by the template identity (Lys, PEG) (2-way ANOVA), indicating that lysozyme templating does not impart specific molecular recognition properties. (Data presented as mean ± SD, n = 3).

Conclusions

The present work determined that polymer composition, not template identity, explains the physical properties, protein adsorption, and molecular recognition ability (i.e. template specificity) of MIPs. We tested protein (varying in MW and pI) and non-protein (PEG, of similar MW) templates, and found that the inclusion of template (up to 5 wt%, in AAm homopolymers or co-polymers containing anionic and hydrophobic components) did not enhance the binding of template to MIPs at equilibrium, relative to NIPs of the same composition. Imprinting did not impart specific template-binding properties in any case.

While it initially appeared that complete template extraction led to an increase in MIPs' protein adsorption, further composition analysis revealed that a chemical change to the polymer backbone explained the difference in lysozyme binding. We determined that protein adsorption was influenced only by chemical changes to the network (i.e. the number of charged and hydrophobic moieties) and not porous architectures generated by specific template inclusion or extraction.

In our analysis, we also measured the macroscopic properties of MIP and NIP networks, such as particle morphology (SEM) and equilibrium weight swelling. Our fabrication process, involving crushing and sieving of particles, resulted in consistent microparticle morphology between formulations. Network composition (i.e. the number of MAA and tBMA groups) significantly influenced the extent of equilibrium swelling in aqueous buffer, but the swelling ratio did not correlate with the model protein adsorption data. This confirmed that the extent to which each MIP or NIP bound a model protein was explained primarily by the number of complementary Coulombic and hydrophobic interactions, and not physical perturbation to molecular transport. These key findings are summarized in **Table 2.**

Table 2: Summary of the impact of each variables tested on the MIPs' swelling ratio, quantity of protein bound, and specific affinity for their template.

Variable	Condition	Swelling Ratio	Protein Absorption	Template Specificity of MIPs
Composition	*Ionizable Monomer*	Increase	Significant increase for all proteins with a complementary net charge	None
	Hydrophobic Monomer	Decrease	Increase for some but not all proteins	None
	Ionic-Hydrophobic Interaction	Similar to hydrophobic in absence of ionic	Synergy observed only for lysozyme	None
Template Identity	*Template MW*	No effect	No effect	None
	Template pI	No effect	No effect	None
	Protein vs. PEG	No effect	No effect	None
Purification Method	*Medium Extraction (EDTA)*	Increase	Increase	None
	Complete Extraction (Trypsin/EDTA)	Increase	Increase	None
Amount of Template	*Before Extraction*	Decrease	Decreases	None
	Complete Extraction	No effect	No effect	None

Our work suggests that the design process for recognitive polymers and networks should focus on the polymerization (monomeric) or fabrication (polymeric) of compatible charged and hydrophobic species, which uniquely engage a protein target. We demonstrated that enhancements in template adsorption, which could have been incorrectly attributed to molecular imprinting, were more suitably explained by chemical alteration of the polymer backbone. Future studies that use molecular imprinting to enhance the affinity of networks for target molecules must measure the extent to which the template is extracted and the network is chemically modified by purification conditions. This rigor must be applied

universally to ensure that the field understands and does not confound the mechanisms underlying the molecular recognition capability of MIPs.

Conflicts of Interest

There are no conflicts of interest to declare.

Acknowledgements

The authors gratefully recognize financial support from the Cockrell Family Chair Foundation, and the National Institutes of Health (NIH) (EB022025 to NAP). AKV was supported by an undergraduate research fellowship from the UT Austin Office of Undergraduate Research. JRC was supported by an NSF Graduate Research Fellowship (DGE-1610403). The authors thank Dwight Romanovicz and Michelle Mikesh from the Institute for Cellular and Molecular Biology at UT Austin for assistance with electron microscopy.

Notes and References

1 J. Z. Hilt and M. E. Byrne, *Adv. Drug Deliv. Rev.*, 2004, **56**, 1599–1620.

2 J. Li and D. J. Mooney, *Nat. Rev. Mater.*, 2016, **1**, 1-17.

3 I. Stanislawska, W. Liwinska, M. Lyp, Z. Stojek and E. Zabost, *Molecules*, 2019, **24**, 1873.

4 H. R. Culver, J. R. Clegg, N. A. Peppas, *Acc. Chem. Res.*, 2018, **50**, 170–178.

5 M. E. Byrne, K. Park and N. A. Peppas, *Adv. Drug Deliv. Rev.*, 2002, **54**, 149–161.

6 M. E. Byrne, K. Park and N. A. Peppas, *MRS Proc.*, 2002, **724**, N9.3.

7 M. J. Whitcombe, I. Chianella, L. Larcombe, S. A. Piletsky, J. Noble, R. Porter and A. Horgan, *Chem. Soc. Rev.*, 2011, **40**, 1547–1571.

8 E. Battista, F. Causa and P. Netti, *Gels*, 2017, **3**, 20.

9 M. R. Gama and C. B. G. Bottoli, *J. Chromatogr. B Anal. Technol. Biomed. Life Sci.*, 2017, **1043**, 107–121.

10 M. I. Neves, P. L. Granja, M. E. Wechsler, N. A. Peppas, M. E. Gomes and R. L. Reis, *Tissue Eng. - Part B Rev.*, 2017, **23**, 27–43.

11 B. V. Slaughter, S. S. Khurshid, O. Z. Fisher, A. Khademhosseini and N. A. Peppas, *Adv. Mater.*, 2009, **21**, 3307–3329.

12 H. R. Culver and N. A. Peppas, *Chem. Mater.*, 2017, **29**, 5753–5761.

13 P. Zahedi, M. Ziaee, M. Abdouss, A. Farazin and B. Mizaikoff, *Polym. Adv. Technol.*, 2016, **27**, 1124–1142.

14 R. Arshady and K. Mosbach, 1981, **692**, 687–692.

15 N. A. Peppas and M. E. Byrne, *Bull. Gattefosse,* 2003, ***96,*** 25–38.

16 S. S. Khurshid, C. E. Schmidt and N. A. Peppas, *J. Biomater. Sci. Polym. Ed.*, 2011, **22**, 343–362.

17 S. Fermani, G. Falini, M. Minnucci and A. Ripamonti, *J. Cryst. Growth*, 2001, **224**, 327–334.

18 J. L. Oncley, G. Scatchard and A. Brown, *J. Phys. Chem.*, 1947, **51**, 184–198.

19 P. G. Righetti, G. Tudor and E. Gianazza, *J. Biochem. Biophys. Methods*, 1982, **6**, 219–227.

20 T. Mary and I. Bassett, *Biochem. J.*, 1980, **191**, 867–868.

21 D. Malamud and J. W. Drysdale, *Anal. Biochem.*, 1978, **86**, 620–647.

22 R. December, *Glass*, 1971, 394–400.

23 M. Graf, R. Galera García and H. Wätzig, *Electrophoresis*, 2005, **26**, 2409–2417.

24 J. R. Clegg, A. S. Irani, E. W. Ander, C. M. Ludolph, A. K. Venkataraman, J. X. Zhong, N. A. Peppas. *Sci. Adv,* 2019, **5**, eaax7946.

25 P. K. Smith, R. I. Krohn, G. T. Hermanson, A. K. Mallia, F. H. Gartner, M. D. Provenzano, E. K. Fujimoto, N. M. Goeke, B. J. Olson, D. C. Klenk, *Anal. Biochem.,* **150**, 76-85.

26 P. Luliński and D. Maclejewska, *Mater. Sci. Eng. C*, 2011, **31**, 281–289.

27 H. Dong, H. Du and X. Qian, *J. Phys. Chem. A*, 2008, **112**, 12687–12694.

28 J. R. Clegg, J. X. Zhong, A. S. Irani, J. Gu, D. S. Spencer and N. A. Peppas, *J. Biomed. Mater. Res. - Part A*, 2017, **105**, 1565–1574.

29 J. X. Zhong, J. R. Clegg, E. W. Ander and N. A. Peppas, *J. Biomed. Mater. Res. - Part A*, 2018, **106**, 1677–1686.

30 J. T. Peters, S. Verghese, D. Subramanian and N. A. Peppas, *Regen. Biomater.*, 2017, **4**, 281–287.

31 E. Axpe, D. Chan, G. S. Offeddu, Y. Chang, D. Merida, H. L. Hernandez and E. A.

Appel, *Macromolecules*, 2019, **52**, 6889–6897.

32 T. Canal and N. A. Peppas, *J. Biomed. Mater. Res.*, 1989, **23**, 1183–1193.

33 S. R. Lustig and N. A. Peppas, *J. Appl. Polym. Sci.*, 1988, **36**, 735–747.

34 M. C. Koetting, J. T. Peters, S. D. Steichen and N. A. Peppas, *Mater. Sci. Eng. R Reports*, 2015, **93**, 1–49.

35 A. G. Mikos and N. A. Peppas, *Biomaterials*, 1988, **9**, 419–423.

36 L. Brannon-Peppas and N. A. Peppas, *Chem. Eng.*, 1991, **46**, 715–722.

37 F. C. Wireko, G. E. Kellogg and D. J. Abraham, *J. Med. Chem.*, 1991, **34**, 758–767.

38 H. R. Culver, S. D. Steichen and N. A. Peppas, *Biomacromolecules*, 2016, **17**, 4045–4053.

39 S. A. Piletsky, H. S. Andersson and I. A. Nicholls, *Macromolecules*, 1999, **32**, 633–636.

40 C. Baggiani, C. Giovannoli, L. Anfossi, C. Passini, P. Baravalle and G. Giraudi, *J. Am. Chem. Soc.*, 2012, **134**, 1513–1518.

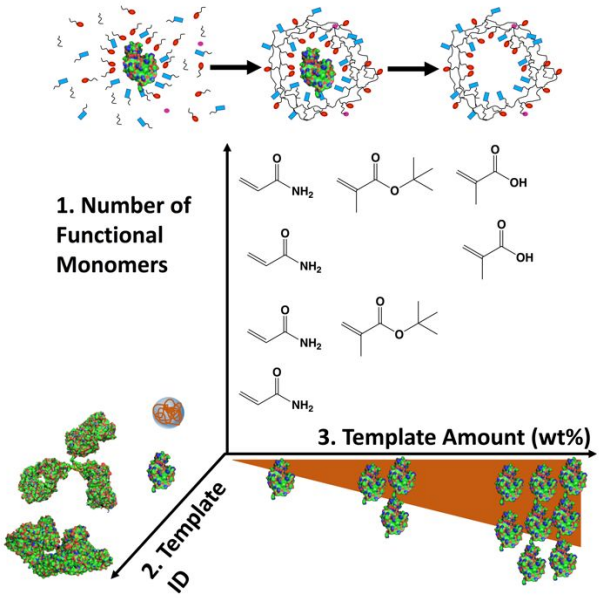

A hydrogel's molecular recognition properties are determined by the material composition, and are minimally influenced by molecular imprinting.